

Photoswitchable phospholipids for the optical control of membrane processes, protein function, and drug delivery

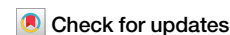
Stefanie D. Pritzl, Johannes Morstein, Nikolaj A. Pritzl, Jan Lipfert, Theobald Lohmüller, Dirk H. Trauner

Angaben zur Veröffentlichung / Publication details:

Pritzl, Stefanie D., Johannes Morstein, Nikolaj A. Pritzl, Jan Lipfert, Theobald Lohmüller, and Dirk H. Trauner. 2025. "Photoswitchable phospholipids for the optical control of membrane processes, protein function, and drug delivery." *Communications Materials* 6 (1): 59. <https://doi.org/10.1038/s43246-025-00773-8>.

<https://doi.org/10.1038/s43246-025-00773-8>

Photoswitchable phospholipids for the optical control of membrane processes, protein function, and drug delivery



Stefanie D. Pritzl¹✉, Johannes Morstein², Nikolaj A. Pritzl¹, Jan Lipfert^{1,3}, Theobald Lohmüller⁴ & Dirk H. Trauner⁵

Recent insights into the function and composition of cell membranes have transformed our understanding from primarily viewing these structures as passive barriers to recognizing them as dynamic entities actively involved in many cellular functions. This review highlights advances in the photopharmacology of phospholipids, emphasizing in particular the role of diacylglycerophospholipids and the impact of their polymorphic nature on synthetic and cellular membrane properties and metabolic processes. We explore photoswitchable diacylglycerophospholipids, termed ‘photolipids’, which permit precise, reversible modifications of membrane properties via light-induced isomerization. The ability to optically switch phospholipid properties has potential applications in controlling membrane dynamics, protein function, and cellular signaling pathways, and offers promising strategies for drug delivery and treatment of diseases. Developments in azobenzene and hemithioindigo based photolipids are discussed, underscoring their utility in biomedical and biomaterial science applications due to their unique photophysical properties.

Historically, the lipid bilayers of cell membranes were viewed primarily as passive barriers and scaffolds for proteins and other components, which were considered the main regulators of cellular activity^{1,2}. Recent research, however, highlights the lipid bilayers’ active role in cell functionality^{3–6}. The cellular lipidome, encompassing thousands of distinct lipids⁷, along with the precise spatial organization and asymmetry of these lipids, significantly influences the membrane’s biophysical properties and lipid-protein interactions^{8–11}. Lipids play a critical role in many physiological processes, such as cellular communication, environmental response, energy transduction and storage, and metabolism^{12–14}. Furthermore, lipid membranes are central to cell protection and compartmentalization.

Dynamic forces within the membrane, including lateral and transverse tension and stress, emerge upon changes, such as bending and stretching, permeability and diffusion, and modifications in lipid composition¹⁵. Variations in the asymmetry and composition of the bilayer’s dual leaflets can significantly alter the functionality of transmembrane channels and peripheral membrane-binding proteins^{15–17}. Simplified lipid membrane model systems, such as vesicles and supported bilayers, replicate the essential features of cellular membranes while reducing complexity¹⁸. These models,

alongside advances in molecular dynamics (MD) simulations¹⁹, are critical for understanding membrane dynamics and functions.

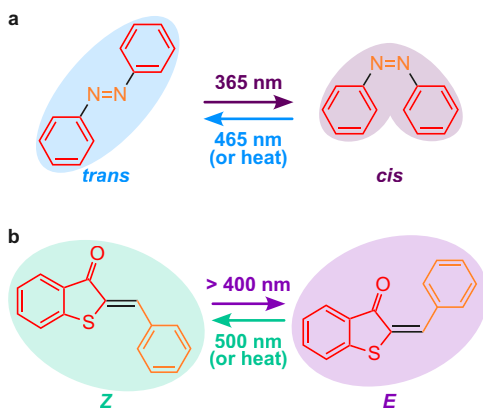
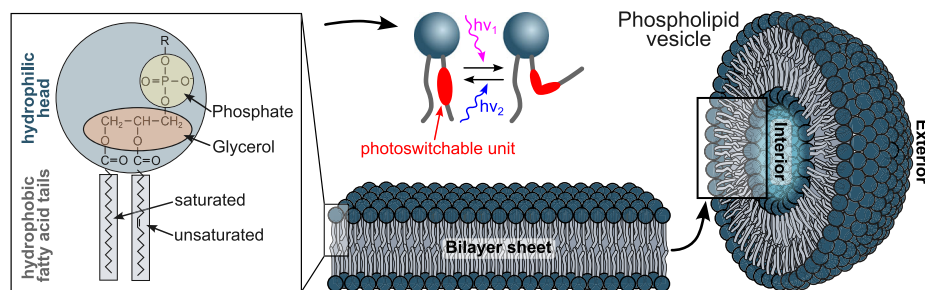
Diacylglycerophospholipids are the most abundant types of structural lipids in cellular membranes²⁰. They consist of a hydrophilic headgroup and two hydrophobic tails, enabling their self-assembly into lipid bilayer structures in an aqueous environment (Fig. 1)²¹. The glycerol backbone of these lipids is attached to fatty acids at the *sn1* and *sn2* positions, and different types of fatty acids cause variability in membrane fluidity and organization. The *sn3* position links to a phosphate with various substituents giving rise to the different glycerophospholipid types such as phosphatidylcholine (PC), phosphatidylethanolamine (PE), phosphatidylserine (PS), and others. Each type contributes distinct characteristics to the membrane, affecting its charge and functional properties based on the headgroup and the surrounding solvent molecules and ions. In addition, polyunsaturated hydrocarbon chains enhance chain disorder and dynamics, including upturns and backfolding, contributing to membrane curvature and lipid domain formation^{22,23}.

A notable example of phospholipid activity is the exposure of PS on the outer leaflet of platelets during blood coagulation²⁴. Normally, PS is on the

¹Soft Condensed Matter and Biophysics, Department of Physics and Debye Institute for Nanomaterials Science, Utrecht University, 3584 CC Utrecht, The Netherlands. ²Division of Chemistry and Chemical Engineering, California Institute of Technology, Pasadena, California, 91125, USA. ³Institute for Physics, Augsburg University, 86159 Augsburg, Germany. ⁴Chair for Photonics and Optoelectronics, Nano-Institute Munich, Department of Physics, Ludwig-Maximilians-Universität (LMU), 80539 Munich, Germany. ⁵Department of Chemistry, College of Arts and Sciences, University of Pennsylvania, Philadelphia, PA, 19104-6323, USA. ✉e-mail: S.D.Pritzl@uu.nl

Fig. 1 | Phospholipids in bilayer membranes.

Phospholipid molecules are composed of a hydrophilic polar phosphate “head” containing the phosphate and glycerol units and two hydrophobic non-polar fatty acid “tails”. Phospholipids are organized into a bilayer sheet, with two layers of molecules arranged tail-to-tail. Within this structure, the hydrophobic tails cluster together away from water, forming the membrane’s interior, while the hydrophilic heads face the aqueous environments inside and outside the vesicle. Photoswitchable phospholipids contain a photoswitchable unit in the hydrophobic tail that can be switched between two conformations upon light exposure.

**Fig. 2 | Photoswitchable molecules used to functionalize phospholipids.**

a Azobenzene consists of two benzene rings (red), linked via a nitrogen double bond (orange). In the *trans* form, it shows a planar structure. The *cis* form is characterized by a twisted geometry. *Trans*-to-*cis* switching is achieved with UV-A light of 365 nm and the back-switch from *cis*-to-*trans* with visible blue light of 465 nm or heat.

b Hemithioindigo photoswitches consist of a thioindigo (red) and a stilbene part (orange). Photoisomerization from the thermodynamically stable *Z* state to the metastable *E* form is possible with purple light of >400 nm, while back-switching is achieved with green light of 500 nm or heat. Tables 1, 2 summarize photoswitchable phospholipids’ chemical structures and photoswitch positions.

inner membrane, but platelet activation disrupts this asymmetry, moving PS outward. This creates a negatively-charged surface essential for forming coagulation complexes and converting prothrombin to thrombin, a vital clotting step. PC, the main phospholipid found in eukaryotic membranes, also plays critical roles. In the lung, dipalmitoylphosphatidylcholine (DPPC) is the main component of pulmonary surfactants, which reduces alveolar surface tension and supports gas exchange²⁵. A lack of DPPC is linked to neonatal respiratory distress syndrome²⁵. PC further promotes the translocation of apolipoprotein B-100 from the cytosol to the endoplasmic reticulum lumen, a crucial early step in the assembly of very low-density lipoproteins²⁶.

Despite their critical roles, the complex polymorphic nature of glycerophospholipids and their impact on cellular functions are not yet fully understood. Dysregulation of glycerophospholipid polymorphism has been linked to various diseases, including lipotoxicity²⁷, psoriasis²⁸, and neurodegenerative disorders^{29–31}.

Emerging research into lipid polymorphism and its biological significance involves the chemical modification of phospholipids, which allows for the exploration and control of distinct structural features and the introduction of new functionality. In particular, photoswitchable lipids offer opportunities for precise and reversible control of lipid and membrane properties^{32,33}. Integrating a photoswitchable motif into the acyl chains of diacylglycerophospholipids allows for transitions between two distinct lipid

geometries upon light irradiation (Fig. 1). Light offers key advantages over other stimuli due to its non-invasive nature and unmatched spatial and temporal resolution³⁴. It allows for targeted modulation of specific cells or regions without impacting surrounding tissues, providing greater control for studying membrane dynamics with minimal disruption. This precision supports more accurate experiments and potentially new forms of therapy with fewer side effects than e.g., traditional small-molecule approaches.

In this review, we examine recent advances in the design and synthesis of photoswitchable diacylglycerophospholipids, termed ‘photolipids’, and their applications in modulating bilayer properties and protein trafficking within both model systems and cellular membranes. By focusing on photoswitchable diacylglycerophospholipids, our review complements previous reports and review articles^{32,33,35–40} that address recent progress using photoswitchable surfactants, fatty acids, peptides, and other molecules and types of lipids. Significant progress has been made with azobenzenes as the photoswitchable unit in diacylglycerophospholipids (Fig. 2a), making them the most studied class of photolipids. Our review focuses on these azobenzene-based systems due to the extensive research available. In addition, we discuss other, less explored, photoswitchable lipids, like hemithioindigo-modified diacylglycerophospholipids (Fig. 2b), hoping to inspire further research. Both azobenzene and hemithioindigo photolipids form stable membranes that preserve reversible *cis*-*trans* isomerization.

Azobenzene-modified diacylglycerophospholipids

Azobenzene, arguably one of the best-studied molecular photoswitches, exhibits a robust and reversible isomerization mechanism⁴¹, which was initially discovered by Hartley⁴² in 1937. Its applications span diverse fields, ranging from energy storage and conversion in polymer science⁴³ to the development of artificial molecular motors and switches in photopharmacology⁴⁴. Parent (unsubstituted) azobenzene consists of two phenyl rings connected by a diazene link and can switch between its *trans* and *cis* isomeric states under the irradiation of blue and ultraviolet (UV)-A light, respectively (Fig. 2a)⁴⁵. The planar *trans* isomer represents the ground state with the benzene rings positioned on opposite sides of the diazene group, whereas the *cis* form features a rotated geometry of the phenyl rings⁴². Thermodynamically, the *trans* configuration is more stable and predominates in thermal equilibrium (quantum yields in low viscosity solvents: $\Phi_{trans \rightarrow cis} = 0.2 - 0.36$ and $\Phi_{cis \rightarrow trans} = 0.4 - 0.69$; ground state energy difference $\Delta E = E(S_0)_{cis} - E(S_0)_{trans} \approx 0.5 - 1\text{eV}$)^{41,46}.

Mechanics of Photoswitching

Azobenzene’s photoswitching involves the excitation of two distinct absorption bands: the $\pi\pi^*$ ($S_0 \rightarrow S_2$) transition around 320 nm, which triggers *trans*-to-*cis* switching, and the $n\pi^*$ ($S_0 \rightarrow S_1$) transition at ~450 nm, which initiates *cis*-to-*trans* isomerization⁴¹. Upon absorption of a photon, energy dissipation leads to azobenzene undergoing in-plane bending and torsion around the N = N axis. While *cis*-to-*trans* switching primarily occurs along the rotation path, the exact mechanism for *trans*-to-*cis* switching remains debated. Recent studies suggest it involves a combination of in-plane bending and rotation, and mechanisms such

as the “hula-twist”⁴⁷, inversion-assisted rotation⁴⁸, and pedal-like interconversions⁴⁹ have been proposed. The dynamics are also influenced by environmental conditions⁴¹, solvent effects⁵⁰, and geometric constraints⁵¹, which determine the specific *cis/trans* ratios at the photostationary states (PSS). Additionally, spin-orbit couplings with azobenzene’s triplet states add complexity to the switching mechanism, allowing for potential thermal switching via these states, as well as sensitized isomerization and photomodulation through energy or charge transfer from aromatic hydrocarbons^{52–55}.

Molecular modifications

Substituting electron-donating or withdrawing groups on the azobenzene rings alters the isomerization wavelengths towards the near IR biological window⁵⁶. Modifications at the *para*-positions can generally enhance switching quantum yields and thermal isomerization rates, with the switching kinetics being influenced by the nature of the substituent and the polarity of the solvent⁵⁷. Conversely, *ortho*-substitution appears to be unaffected by the solution conditions⁵⁶. Notably, tetra-*ortho*-substitution on azobenzene derivatives, such as tetra-*ortho*-methoxy substitution or tetra-*ortho*-fluorination, extends isomerization wavelengths into the red or far-red spectrum, and significantly enhance the thermal stability of the *cis* isomer from days to years^{38,58}. Employing chlorine as a substituent further shifts the isomerization wavelengths towards red, facilitating *trans*-to-*cis* switching with red light around 660 nm⁵⁹.

Synthesis routes of azobenzene photolipids

A variety of azobenzene-modified diacylglycerophospholipids have been reported (Table 1). Synthetic strategies for phosphocholine derivatives encompass (i) acylation of lysophospholipids using a mixed anhydride prepared from a purified photoswitchable fatty acid (Ao8EPC, 6Ao8EPC, Ao8,6Ao2EPC, 6A4EPC, **dazo-PC**, *azo-PC*)^{60–62} or Yamaguchi esterification to install the fatty acid FAAzo-4 (*azo-PC* and **dazo-PC**)^{63,64} or the red-shifted fatty acid red-FAAzo-4⁶⁵ (**red-azo-PC**), (ii) phosphoramidite chemistry to attach the headgroup to a photoswitchable diacylglycerol (*azo-PC*)⁶⁶, and (iii) successive assembly of the lipid tail on a diacylglycerophospholipid (tetra-*ortho*-fluoro azobenzene-based relay transporter)⁶⁷. Phosphatic acid derivatives were synthesized via (i) phosphorylation of PhoDAG-1 with a phosphoramidite, subsequent oxidation, and protecting group cleavage with trifluoroacetic acid (TFA) (AzoPA)⁶⁸, or via (ii) acylation of a protected form of AzoLPA with FAAzo-4 and subsequent deprotection with TFA (dAzoPA)⁶⁸. In addition, diacylglycerophospholipid mimics were synthesized via an Arbuzov reaction (Azo-9P, 4-Azo-6P, 4-Azo-5P, DT 5Azo)^{69–72}. Although these mimics are not diacylglycerophospholipids due to the absence of the glycerol unit, we included them as they were designed to mimic membrane diacylglycerophospholipids.

Early studies of azobenzene-containing photolipid membrane systems

The first reports of photoswitchable diacylglycerophospholipid derivatives emerged in the 1980s. In 1985, Morgan et al. introduced the synthesis of *azo-PC*, a photoswitchable phospholipid with an azobenzene unit embedded in one of the acyl chains⁶². In their foundational study, they prepared vesicle mixtures comprising 1,2-dipalmitoyl-*sn*-glycero-3-phosphocholine (DPPC) and *azo-PC* and discovered that the photoswitching efficiency in the DPPC/*azo-PC* vesicle mixtures, i.e., reversibility of the *trans* and *cis* absorption spectra after cycled photoisomerization, is preserved and comparable to that of *azo-PC* in ethanolic solutions, demonstrating that azobenzene photoisomerization remains effective within the lipid host matrix. Using light scattering and fluorescence spectroscopy, the study also showed that *cis-trans* isomerization significantly impacts membrane permeability and osmotic shrinkage. Vesicles containing the *trans-azo-PC* could encapsulate solutes and maintain a pH gradient across the bilayer until switched to the *cis* form, which increased membrane permeability to water and ions.

In 1986, Sandhu et al. used Langmuir-Blodgett and light scattering techniques and observed that mono-azobenzene-containing phospholipids

like *azo-PC*, palmitoyl *azo-PC*, and oleoyl *azo-PC*, as well as **dazo-PC** with two azobenzene units alter the area per lipid (Fig. 3a) and decrease membrane rigidity when transitioning from *trans*-to-*cis*⁶⁰. *Trans-dazo-PC* samples exhibited a distinct phase transition in contrast to *azo-PC*, indicating high packing cooperativity. Further light-scattering and fluorescence spectroscopy studies supported a highly cooperative phase behavior exclusive to **dazo-PC**⁷³. Additionally, an increase in motional freedom and membrane fluidity post *trans*-to-*cis* isomerization was noted⁷³, alongside a significant hypsochromic shift in the main absorption peak of *trans* photolipids in a membrane setting compared to monomeric photolipids in chloroform⁶¹. This shift was consistent with enhanced transition dipole interactions and H-aggregate formation (Fig. 3b), as explored by Song et al., who documented H-aggregation in pure and mixed photolipid vesicle dispersions, accompanied by induced circular dichroism⁶¹.

Subsequent studies focused on understanding and controlling photo-induced solute release and liposome fusion under various conditions, applying different experimental assays, in particular fluorescence polarization and spectroscopy, absorption spectroscopy, electron microscopy, and differential scanning calorimetry^{61,69,74–81}. A comparative study revealed that lower concentrations of **dazo-PC** were required compared to *azo-PC* to trigger cargo release from vesicles and promote liposome fusion or lipid exchange after *trans*-to-*cis* isomerization^{74,75}. Moreover, the addition of cholesterol to *cis*-azobenzene-containing vesicles enabled step-wise, wavelength-dependent control of solute release^{76,77}, and the use of short intense laser pulses and heat could even accelerate the process^{78,79}. However, host matrices in a liquid-crystalline phase or composed of unsaturated acyl chains, and the absence of H-aggregation, could inhibit cargo release at low *cis-dazo-PC* levels^{61,75,77}. Notably, successful leakage from photolipid/1,2-dioleoyl-*sn*-glycero-3-phosphocholine (DOPC) vesicles required concentrations of *cis-dazo-PC* of 20 mol% or more⁶⁹. Early experiments also successfully encapsulated antitumor drugs like methotrexate⁸⁰ and cupric ions⁸¹, the latter catalyzing the autoxidation of ascorbate and epinephrine upon release, demonstrating the potential of photosensitive liposomes as drug delivery vehicles for photodynamic therapy.

To date, most research has focused on lipid mixtures containing up to 40 mol% of photolipids, with **dazo-PC** being the most extensively studied variant for triggering permeability and fusion. Investigations of model membrane systems composed solely of photolipids have been limited, partly due to synthesis routes that not only require many steps but also result in only low yields and often heterogeneous (azobenzene incorporation in the *sn1* or *sn2* positions) photolipid products⁶². Studying pure photolipid membranes and, thus, the pure switching mechanism in a membrane setting without contributions from standard non-switchable lipids could provide deeper insights into the interactions and membrane properties, particularly the mechanisms underlying cargo release and liposome fusion, which remained unclear, especially for the reverse *cis*-to-*trans* switching directions. Morgan et al. further suggested the existence of locally disordered regions and channel formation as a potential mechanism for fusion with **dazo-PC**/DPPC vesicle mixtures⁷⁴, but clear evidence is missing.

Pure photolipid model membrane systems—pushing the limits

Recent advances in synthesizing large quantities of homogenous photolipids through more efficient synthetic routes have made it feasible to prepare pure photolipid model membranes. These systems range from monolayers at air/water interfaces to supported lipid bilayers and vesicles varying from ~100 nm to several micrometers in diameter^{66,71,82}.

In 2011, Backus et al. prepared pure photolipid monolayers of negatively-charged DT Azo-5P at an air/water interface and examined their molecular properties using vibrational sum-frequency generation spectroscopy (VSFG)⁷¹. They not only confirmed the increase in lipid area upon *trans*-to-*cis* switching, previously reported by ref. 60, but also revealed that the dipole moment of the *cis* isomer favors interactions with water (Fig. 4a). High surface pressure coupled with a low VSFG signal suggested a reduction in surface free energy via electrostatic interactions between lipid headgroups

and water molecules. The electrostatic interaction seemingly reduces the effect of the headgroups' negative charge, leading to loop formation in the lipid tails and decreased molecular order. Similar effects were found in charge-neutral photolipid *azo-PC*^{82–84}, where a reduced molecular order of *cis* lipids resulted in decreased membrane thickness and increased vesicle

size^{66,82–84}. For example, small angle X-ray⁸² and dynamic light scattering⁶⁶ measurements revealed head-to-head distances of $d_{HH}^{cis} \approx 34 \text{ \AA}$ and $d_{HH}^{trans} \approx 39 \text{ \AA}$ and vesicle diameters of $D_{cis} \approx 124.3 \text{ nm}$ and $D_{trans} \approx 120.5 \text{ nm}$, respectively. Additionally, stronger water interactions with *cis* isomers agree with simulations for photoswitchable fatty acid FAAzo-4 and *azo-PC*,

Table 1 | Azobenzene-modified phospholipids

Name	Chemical structure	Reported effects
Ao ₈ EPC		H-aggregates, circular dichroism, and solute release ⁶¹
₆ Ao ₈ EPC		H-aggregates, circular dichroism, and solute release ⁶¹
Ao _{8,6} Ao ₂ EPC		H-aggregates, circular dichroism, and solute release ⁶¹
AzoPC/ <i>azo-PC</i>		Stiffness ^{66,86} , thickness ^{82,86,91} , membrane area ⁸⁶ , area per lipid ^{83,84} , engulfment ⁹⁰ , vesicle size ⁶⁶ , fluidity ⁸² , solute release ^{84,86,96,97} , H-aggregates ^{64,82} , fusion ^{63,89} , toxicity ⁹⁶ , protein response and CH ordering effect ⁸⁸ , solvent effects ⁹¹ , phase separation ⁶⁴ , protein secretion (also for C16 derivative) ⁹⁵
Bis-AzoPC / <i>dazo-PC</i> / ₄ A ₄ EPC		Fusion ^{63,74,75} , permeability ^{61,82,74,76,79} , solute release ^{62,76–78,81} , H-aggregates ^{61,63} , circular dichroism ⁶¹ , membrane phase state ^{60,73} , fluidity ^{63,73} , stiffness ⁶³ , phase separation ⁶³
AzoPA		Signalling of mTOR and Hippo ⁶⁸
dAzoPA		Signalling of mTOR and Hippo ⁶⁸
<i>red-azo-PC</i>		Stiffness ⁶⁵ , fusion ⁶⁵ , fluidity ⁶⁵ , vesicle size ⁶⁵ , thickness ⁶⁵ , permeability ^{65,96} , toxicity ⁹⁶
Tetra-ortho-fluoro- azo-PC		Ion transport ⁶⁷

Table 1 (continued) | Azobenzene-modified phospholipids

Name	Chemical structure	Reported effects
DT Azo-5P/ 4-Azo-5P		Surface pressure and molecular ordering ⁷¹ , MscL activation ⁷² , H-aggregation ⁶⁹
Azo-9P		H-aggregation ⁶⁹
4-Azo-6P		H-aggregation ⁶⁹

Names and chemical structures of the reported *trans*-azobenzene-modified diacylglycerophospholipids and phospholipid mimics, and their applications.

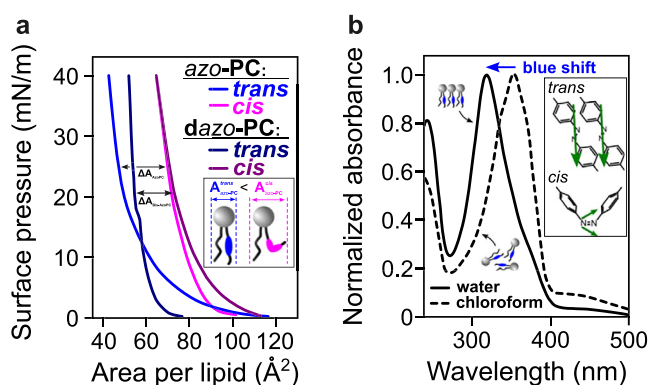


Fig. 3 | Early photolipid characterizations. **a** Surface pressure/area isotherms for compression of *azo*-PC and *dazo*-PC in the *trans* (blue) and *cis* (purple) state. For both photolipids, the area per *cis* lipid is larger than the area per *trans* lipid at surface pressures > 3 mN/m. The ‘knee’ region in the isotherm of *dazo*-PC indicates gel/fluid phase equilibrium. Adapted from ref. 60. **b** Absorbance spectra of Azo8EPC in water (solid line) and chloroform (dashed line). The blue-shifted absorbance of Azo8EPC in water compared to chloroform indicates H-aggregate formation. Adapted from ref. 61. Inset: Schematic of transition dipole moments for *trans* and *cis* azobenzene. In bilayer geometry, *trans* azobenzene molecules have their transition dipoles (green arrows) aligned parallel to the bilayer plane. The *cis* form can adopt two possible orientations of its transition dipole moment. The data were re-plotted from the original publications.

suggesting energetically more favorable hydrophilic interactions and water access to the central N = N bond for *cis* than *trans* isomers⁸⁵, as well as ~3.5 times larger water permeation coefficients of *cis*-*azo*-PC giant unilamellar vesicles (GUVs) than *trans* photolipid vesicles ($P_{cis}^{water} \approx 39 \mu\text{m s}^{-1}$ and $P_{trans}^{water} \approx 11 \mu\text{m s}^{-1}$)⁸⁶.

Altogether, these findings support the hypothesis that changes in lipid area and compressibility during isomerization increase membrane permeability through transient pore formation, confirmed through leakage experiments with dye-loaded photolipid vesicles (Fig. 4b) and patch-clamp measurements on free-standing lipid bilayers⁸⁷. Interestingly, a rapid and substantial reduction in the area upon switching back from *cis* to *trans* resulted in almost instantaneous vesicle depletion, a phenomenon explainable by a rapid reduction of the lipid area due to faster dynamics in *cis*-to-*trans* photoswitching⁸⁷. Moreover, the pronounced defect formation and varying molecular order of *trans/cis* isomers are most evident in pure photolipid membranes and diminish in the presence of non-switchable lipids such as 1,2-diphytanoyl-*sn*-glycero-3-phosphocholine (DPhPC) or DPPC^{64,66,71,83,86}. In addition, *azo*-PC containing liposomes were characterized by solid-state nuclear magnetic resonance (NMR), showing a UV-light-induced *trans*-to-*cis* isomerization that reduced CH order parameters in lipid acyl chains and increased molecular dynamics⁸⁸.

Furthermore, the high molecular order of *trans* membranes is related to H-aggregation among the *trans* azobenzene units, which results in a pronounced hypsochromic shift of the maximum absorbance peak compared to monomeric *trans* photolipids^{61,64,69}. H-aggregation diminishes when mixed with DPhPC or DOPC and is absent in *cis* membranes, because an increase of the mol fractions of DPhPC or DOPC was shown to reverse the hypsochromic shift while no difference of the absorbance properties between free *cis* molecules and *cis* membranes was observed^{61,66}. Additionally, the introduction of cholesterol into *azo*-PC/DPhPC mixtures leads to phase separation and domain formation of ternary cholesterol/*trans*-*azo*-PC/DPhPC membrane systems, a phenomenon not observed with *cis* isomers (Fig. 4c). The domain size is dependent on the isomerization rate and associated *cis/trans* ratios allowing for dynamic domain growth or shrinkage⁶⁴ and can be further controlled by adjusting the photolipid content, as demonstrated by the post-synthetic incorporation of *dazo*-PC molecules into non-switchable vesicle membranes⁶³.

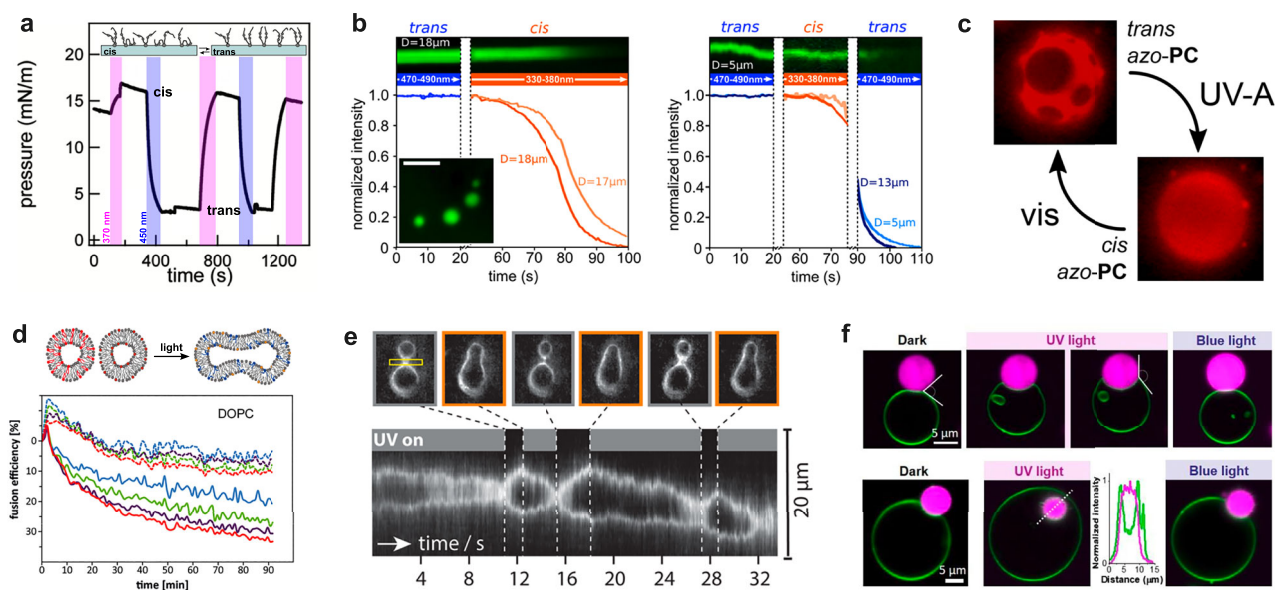


Fig. 4 | Optical control of membrane properties. **a** Surface pressure over time of a monolayer of the photoswitchable phospholipid mimics 4-Azo-5P at the lipid/water interface. Irradiation with 370 and 450 nm light for approximately 100 s (blue/pink bars) induced the high-pressure *cis* state and low-pressure *trans* state, respectively. The minor, sharp fluctuations observed in the pressure data were attributed to adjustments in the sample height to compensate for water evaporation. Reprinted (adapted) with permission from *J. Phys. Chem. B* 2011, 115, 10, 2294–2302⁷¹. Copyright 2011 American Chemical Society. **b** Release of Atto532 dye molecules from pure *azo-PC* GUVs. Inset: A microscope image of dye-loaded *azo-PC* vesicles (scale bar: 20 μm). Left side: Photoswitching the molecules in the vesicle membrane from *trans* (blue solid lines) to *cis* (orange solid lines) using UV-A light results in a decrease in fluorescence over time, as depicted in the kymograph of a vesicle with an 18- μm diameter. Right side: Subsequent illumination with blue light, which switches the photolipids back to *trans* (light blue solid lines), leads to a further reduction in fluorescence. The interruption in the time series corresponds to the time required to change the excitation wavelengths. Reprinted (adapted) with permission from *Langmuir* 2020, 36, 45, 13509–13515⁸⁴. Copyright 2020 American Chemical Society. **c** Domain formation and phase separation occur in ternary *trans-azo-PC*/DPhPC/cholesterol vesicle systems that disappear upon switching to *cis*. Reprinted (adapted) with permission from *Langmuir* 2018, 34, 44, 13368–13374⁶⁴. Copyright 2018

American Chemical Society. **d** Light-induced *azo-PC* isomerization and membrane fusion. Top: Schematic of photo-triggered vesicle fusion. Photoswitching from *trans*-to-*cis* results in lipid splay and subsequent fusion of the vesicles. Bottom: Averaged kinetics of total lipid mixing after combining sonicated DOPC liposomes, which contain varying concentrations of *azo-PC* at a 4:1 ratio, with DOPC liposomes that include 0.8 mol% NBD-PE. NBD fluorescence was monitored over time at 37 $^{\circ}\text{C}$, following UV irradiation (+UV, solid lines) or in the absence of UV light (–UV, dashed lines). Reprinted (adapted) with permission from *BBA Biomembranes* 2020, 1862, 11, 183438⁸⁹. Copyright 2020 Elsevier. **e** The kymograph shows the reversible photocontrol of a vesicle budding transition via *cis-trans* isomerization of giant *azo-PC* vesicles. Reprinted (adapted) with permission from *Langmuir* 2017, 33, 16, 4083–4089⁶⁶. Copyright 2017 American Chemical Society. **f** Light-induced engulfment of protein (glycinin) condensates. The light-induced engulfment of condensates varies with condensate size: large condensates are partially engulfed, while small condensates are fully engulfed. For smaller condensates, photoisomerization creates sufficient excess membrane area for complete, reversible engulfment. The intensity profile along the white dashed line in the neighboring image (left) shows the condensate (magenta line) wrapped by the membrane (green line). Adapted from Mangiarotti et al., *Adv. Sci.* 2024, 2309864⁹⁰.

Consequently, *cis*-to-*trans* isomerization in cholesterol-doped vesicle membranes, followed by rapid area reduction in ordered *trans* domains, can cause fluctuations in the membrane area and the formation of transient membrane voids. This interpretation potentially explains the observed *cis*-to-*trans* photo-triggered solute release from *dazo-PC*/DPPC vesicles upon cholesterol addition, as documented by refs. 76,77.

The changes in molecular footprint and membrane order upon *cis-trans* isomerization also impact membrane stiffness and fluidity, as well as vesicle fusion and engulfment. Reports indicate a decrease in membrane stiffness by one to three orders of magnitude^{64,66,86}, potentially leading to changes in vesicle shape⁶⁶, while an increase in membrane mobility by a factor of two was observed when switching *azo-PC* lipids from *trans*-to-*cis*⁸². Micropipette aspiration experiments of label-free *azo-PC* giant unilamellar vesicles (GUVs) revealed bending moduli of $\kappa_{trans} = 3.1 \cdot 10^{-20}$ J and $\kappa_{cis} = 6.4 \cdot 10^{-21}$ J⁶⁴, while diffusion coefficients for *trans*- and *cis-azo-PC* supported lipid bilayers (SLB) of $D_{trans} = 0.47 \pm 0.04 \mu\text{m}^2 \text{s}^{-1}$ and $D_{cis} = 0.83 \pm 0.06 \mu\text{m}^2 \text{s}^{-1}$ were reported using fluorescence-recovery after photobleaching (FRAP)⁸². The changes in membrane stiffness and fluidity point to a structural phase transition and H-aggregate melting due to changes in area per lipid and membrane order^{64,66,82,84}. H-aggregate melting was concluded from temperature-dependent FRAP measurements, revealing an increase of *trans* membrane fluidity with the temperature that was not observed in *cis* bilayers⁸². In contrast, *dazo-PC* membranes displayed a clear phase transition⁶⁰ and lower diffusion

coefficients⁶³ in *trans* membranes compared to *azo-PC*. Finally, photo-triggered area fluctuations⁶³ and lipid splay⁸⁹ are also suggested to promote vesicle shape changes and fusion⁶³, and lipid mixing⁸⁹ (Fig. 4d, e). Combined theoretical and confocal microscopy studies further suggest that the interaction mechanisms between protein condensates and lipid membranes, i.e., gain in adhesion energy upon *trans*-to-*cis* switching and subsequent variations of the condensate/vesicle contact angle, result in engulfment (Fig. 4f)⁹⁰.

Taken together, these studies not only address questions posed in early research but also demonstrate the broad potential of photolipids for intrinsic optical control of bilayer membrane properties. However, the UV light required for activating unsubstituted azobenzene units in photolipids can damage cells and limits in vivo applications due to tissue absorption and scattering. Photolipids activated by visible or near-infrared light, such as tetra-*ortho*-chlorinated or -fluorinated variants, could be more suitable for biocompatible applications. For instance, *red-azo-PC*, a tetra-*ortho*-chlorinated photolipid that can be switched from *trans*-to-*cis* with red light ≥ 630 nm, exhibits similar effects on membrane rigidity, fluidity, aggregation, and vesicle fusion as its unsubstituted counterparts⁶⁵. Furthermore, tetra-*ortho*-fluorinated photolipids equipped with a transporter relay unit have enabled active control of anion transport across vesicle membranes through light exposure and photoisomerization, demonstrating a novel method for actively transferring anions between bilayer leaflets (Fig. 5)⁶⁷.

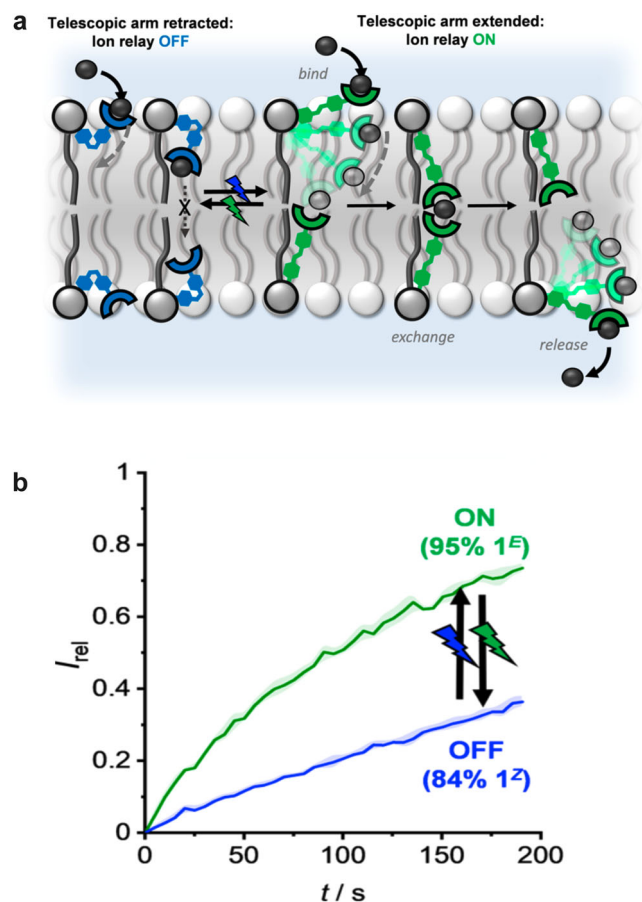


Fig. 5 | Photo-responsive transmembrane anion transporter relay. **a** The system is controlled by manipulating photoswitchable lipids that act as “telescopic arms” of molecular machine-like transporters embedded within the membrane. In the retracted position, the anion-binding arms are unable to exchange ions, maintaining the relay in the OFF state. Upon photo-irradiation, the transporter arms extend, enabling ion exchange between the transporters on opposite sides of the membrane, thus activating the ON state. An electron-deficient aryl-thiourea was used as an effective hydrogen-bonding anion-binding group to promote anion complexation and facilitate membrane entry. **b** Large vesicles containing *trans* anion transporters were loaded with the fluorescent pH indicator 8-hydroxypyrene-1,3,6-trisulfonate (HTPS) and exposed to light (530 nm/405 nm) to generate *cis*- and *trans*-rich PSSs, respectively. The different increases in the relative fluorescence indicate that ion transport across the vesicle membrane was significantly reduced in the *cis*-rich state compared to the *trans*-rich PSS. Reprinted (adapted) with permission from *J. Am. Chem. Soc.* 2022, 144, 23, 10455–10461⁶⁷. Copyright 2022 American Chemical Society under license CC-BY 4.0.

Caveats for the comparison of reported photophysical properties

While the findings are conceptually consistent, quantitative variations of the optical membrane control, i.e., impacts on the photoswitching behavior and reachable PSS and the overall degree of photocontrol, can arise for several reasons:

- Chemical variability:** The headgroups and acyl chains of the various photolipid derivatives differ in structure, composition, and charge. For instance, H-aggregation is enhanced by increasing the proportion of photolipids in the hydrophobic bilayer region, as shown when using *dazo-PC* instead of *azo-PC*^{63,66}. Additionally, electrostatic interactions between lipid headgroups and water molecules can counteract the charge effects of the headgroups⁷¹.
- Solvent effects:** Solvent conditions significantly impact the photostationary state (PSS). Ober et al. demonstrated that using phosphate-buffered saline (PBS) instead of deionized water could double the range of optical control between *trans*- and *cis*-dominant PSS⁹¹.

- Environmental conditions:** Factors such as illumination intensity and power, switching wavelength, and temperature affect *cis-trans* photoisomerization, particularly its kinetics and PSS^{65,82,84,91}. For example, increasing light source power densities accelerates vesicle switching kinetics significantly, while dual-wavelength switching with blue and green light enables fine-tuning of specific *cis/trans* ratios^{82,84}.
- Bilayer setting:** The assembly of photolipids into a bilayer membrane setting can restrict isomerization to a pure *trans* or *cis* PSS, as observed with *azo-PC* and *dazo-PC*^{63,64}.
- Photosensitized switching:** Photosensitization effects must be considered when using dye molecules and fluorescent lipid analogs in photolipid membrane systems for fluorescence-based microscopy studies, even in the absence of spectral overlap between photolipid absorption and fluorophore emission. For instance, the mixing of *azo-PC* and TexasRed™ 1,2-dihexadecanoyl-*sn*-glycero-3-phosphoethanolamine (DHPE) enabled sensitized isomerization of photolipids via resonant excitation of the TexasRed dye, altering the *cis-to-trans* switching kinetics and *trans* and *cis* PSS⁹².
- Sample quality:** Pure and high quality photolipid samples are critical to achieve experimental reliability and reproducibility, because residual detergents and contaminations can impact the switching behavior and membrane response.

Given these factors, a quantitative comparison of existing photolipid studies requires careful consideration of the exact experimental conditions and chemical characteristics of the photolipid derivatives. For example, comparing the size of *azo-PC* and *red-azo-PC* vesicles without emphasizing their difference in chemical structure⁹³, is not advisable. Chlorine substitution in azobenzenes induces an out-of-plane twist of the phenyl rings and a distortion of the CNNC and CCNN angles, resulting in a bulkier molecular geometry compared to unsubstituted azobenzenes⁹³. Also, variabilities in reported membrane compressibility of *azo-PC* were noted⁹³; however, changes in illumination and sample preparation conditions have been shown to cause quantitative differences in *azo-PC* pressure profiles⁸³. Furthermore, the fluid nature of *trans azo-PC* membranes⁹³ is clearly affected by the presence of H-aggregation and dipole-dipole interactions, which was observed in numerous studies^{61,63,64,69}.

In summary, investigations of pure and mixed photolipid model membrane systems have provided a detailed understanding of intrinsic photolipid characteristics and membrane properties. Yet, their full potential for e.g., biological and medical applications in photopharmacology will only be realized through the study of more complex and realistic systems.

Photolipids in complex membrane systems: controlling protein function and secretion with light

Several studies have explored the impact of photolipid isomerization on the activation and signaling of membrane proteins. Notably, incorporation of the mechanosensitive channel of large conductance (MscL)—which responds to membrane tension via pore opening⁹⁴—into vesicle/nanodisc membranes composed of DOPC or DPhPC and 4-Azo-5P⁷² or *azo-PC*⁸³, resulted in channel activation upon *cis-to-trans* isomerization using blue light (Fig. 6a, b). This activation is attributed to changes in the lateral pressure profile induced by photoisomerization, causing structural modifications in MscL’s α -helices.

Furthermore, a recent proof-of-concept study revealed that protein reconstitution into a photolipid *azo-PC* membrane and subsequent photoswitching increases lipid crowding, subsequently reducing lipid diffusion⁸⁸. This alteration prolongs the residence time of proteins near photolipids, making them more responsive to photoisomerization. For instance, the enzyme diacylglycerol kinase (DgkA), responsible for converting diacylglycerol to phosphatidic acid, exhibited increased mobility due to decreased lateral pressure following photoisomerization, demonstrating the tight linkage between protein and membrane dynamics⁸⁸.

The effects of *cis-trans* isomerization of photolipids on cellular signaling pathways and protein secretion have also been investigated directly in live cells. To evaluate the potential of photolipids to regulate critical cell signaling

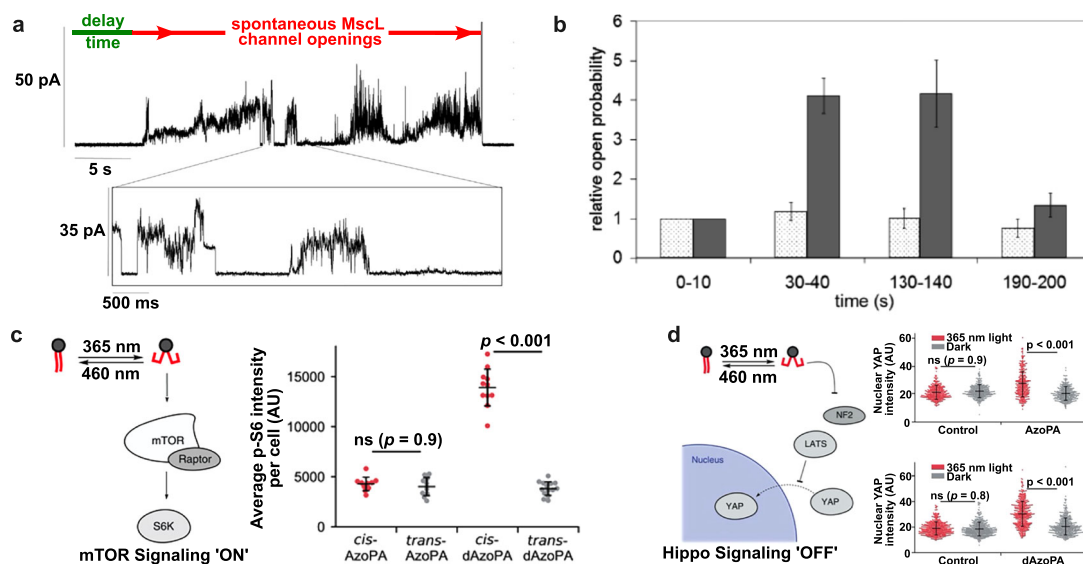


Fig. 6 | Optical control of membrane protein function and secretion via photolipid isomerization. **a** Current traces of MscL activation. MscL were reconstituted in binary lipid membranes of 20% azo-PC and 80% DPhPC. After *cis*-to-*trans* switching with blue light of 455 nm and a delay time of 5 s (green bar), spontaneous openings of the channel were observed (red arrow). Reprinted (adapted) with permission from *Front. Mol. Biosci.*, 9, 2022⁸³. Copyright © 2022 Crea, Vorkas, Redlich, Cruz, Shi, Trauner, Lange, Schlesinger and Heberle. **b** Quantification of the increase of the mean relative open probability of MscL upon *trans* (dotted bars) to *cis* (gray bars) isomerization of 4-Azo-5P: 30–40 s and 130–140 s of illumination at 365 nm and subsequent 50 s illumination at 436 nm (190–200 s). The open probability of the MscL channel from 0 to 10 s was indexed at 1. Error bars indicate the standard error of the mean. Reprinted (adapted) with permission from *Langmuir* 2004, 20, 17, 6985–6987⁷². Copyright 2004 American Chemical Society. **c** Selective activation of mTOR signaling in the presence of photolipids (Azo- and dAzo phosphatidic acids). Left: Diagram illustrating mTOR signaling through activation of the key downstream target p70-S6 kinase (mTORC1). The activation of mTORC1 was evaluated by measuring levels of S6K phosphorylated at Thr389 (p-S6K) using Western blot analysis. Right: Quantification of immunofluorescence analysis, showing the average p-S6 intensity per Serum-starved NIH 3T3 cell. Black horizontal bars represent the mean ($n = 10–14$), with vertical error bars indicating

standard deviation. Statistical significance was determined using one-way ANOVA, followed by Tukey's HSD test. Cells treated with *cis*-dAzoPA exhibited a substantial increase in p-S6 levels. Notably, these effects were specific to dAzoPA and not AzoPA, indicating a high degree of acyl chain selectivity in PA-induced mTOR signaling activity. Reprinted (adapted) with permission from *CS Cent. Sci.* 2021, 7, 7, 1205–1215⁶⁸. Copyright 2021 American Chemical Society under license CC-BY-NC-ND 4.0. **d** Optical control of Hippo signaling in NIH 3T3 cells. Left: Schematic representation of the optical control of Hippo deactivation induced by phosphatidic acid (PA). When Hippo signaling is active, LATS1/2 kinases phosphorylate the transcription factor YAP, preventing its translocation to the nucleus. PA can bind to both LATS1/2 and the upstream factor NF2, inhibiting Hippo signaling. Right: Quantification of nuclear YAP levels. The plots show the mean nuclear YAP intensity per cell. Black horizontal bars represent the mean ($n = 342$ (upper plot) and 465 (lower plot)), with vertical error bars indicating standard deviation. Statistical significance was again determined using one-way ANOVA followed by Tukey's HSD test. Notably, both *cis*-AzoPA and *cis*-dAzoPA, but not their *trans* isomers, induced nuclear translocation of YAP. Reprinted (adapted) with permission from *ACS Cent. Sci.* 2021, 7, 7, 1205–1215⁶⁸. Copyright 2021 American Chemical Society under license CC-BY-NC-ND 4.0.

pathways such as the mammalian target of rapamycin (mTOR) and Hippo, which govern cell growth and proliferation, two photoswitchable phosphatidic acid analogs—AzoPA and dAzoPA—were developed⁶⁸. Following incubation with NIH 3T3 mouse embryonic fibroblast cells for approximately one hour, *trans*-to-*cis* isomerization of these analogs was shown to activate and inhibit mTOR and Hippo signaling, respectively, enabling reversible optical control over these pathways and selective activation (Fig. 6c, d).

Another study has highlighted the rapid uptake of photoswitchable fatty acid (FAAzo-4) by mammalian cells, leading to the production of photoswitchable PC analogs (azo-PC) within the endoplasmic reticulum (ER)⁹⁵. Subsequent irradiation triggered rapid photoisomerization, enhancing membrane fluidity. This increase in fluidity facilitated accelerated protein cargo accumulation at ER exit sites (ERES), subsequently slowing the export rate of cargo from the ERES to the Golgi.

Photolipid vesicles as drug delivery vehicles and magnetic resonance imaging (MRI) sensors

The concept of using photolipid vesicles as drug delivery vehicles was initially suggested in the late 1980s⁹⁰. Recent advancements in lipid nanoparticle and liposome design, coupled with a deeper understanding of *cis*-*trans* isomerization within lipid membranes, have paved the way for innovative strategies that enable precise optical control of localized, dose-dependent drug release *in situ*.

Successful on-demand cargo release has been demonstrated *in cellulo*/*vivo* with the antibiotic doxorubicin (Dox)⁹⁶ and the dopamine D1-receptor

agonist SFK-81297⁹⁷, using lipid nanoparticles (LNPs) doped with azo-PC or red-azo-PC, and azosomes, i.e., nanovesicles containing azo-PC. These studies confirmed the maintenance of biological cargo activity and efficient cellular uptake, without toxic side effects or indications of cell death. Moreover, they are not purely conceptual; photo-triggered cargo release has been investigated *in cellulo*, moving towards clinical relevance. For instance, the photo-triggered release of SFK-81297 from azosomes elevated intracellular Ca^{2+} concentration after D1-receptor activation in primary mouse striatal neurons⁹⁷. Additionally, the doxorubicin-loaded photoactivatable LNPs (paLNPs) were used in zebrafish embryos, demonstrating prolonged blood circulation and extravasation comparable to clinically approved formulations, with enhanced drug release following pulsed light irradiation (Fig. 7)⁹⁶. The paLNPs closely replicate the properties of clinically approved LNPs, with the additional advantage of light-induced drug release, making them promising candidates for clinical development.

Notably, photolipid vesicles loaded with Gadoteridol⁹⁸, a gadolinium-based MRI contrast agent, demonstrated their potential as dynamic MRI sensors *in vivo*, with *trans*-to-*cis* switching boosting water permeability and enhancing MRI signals. The loaded LNPs were successfully injected into live rat brains, targeting striatal tissue near an implanted 200- μ m-diameter optical fiber, akin to devices widely used in optogenetics, photometry, and phototherapy.

Photolipid vesicles hold significant promise as drug delivery and sensing systems. However, their use and study have been predominantly confined to laboratory settings. Consequently, further research is essential to

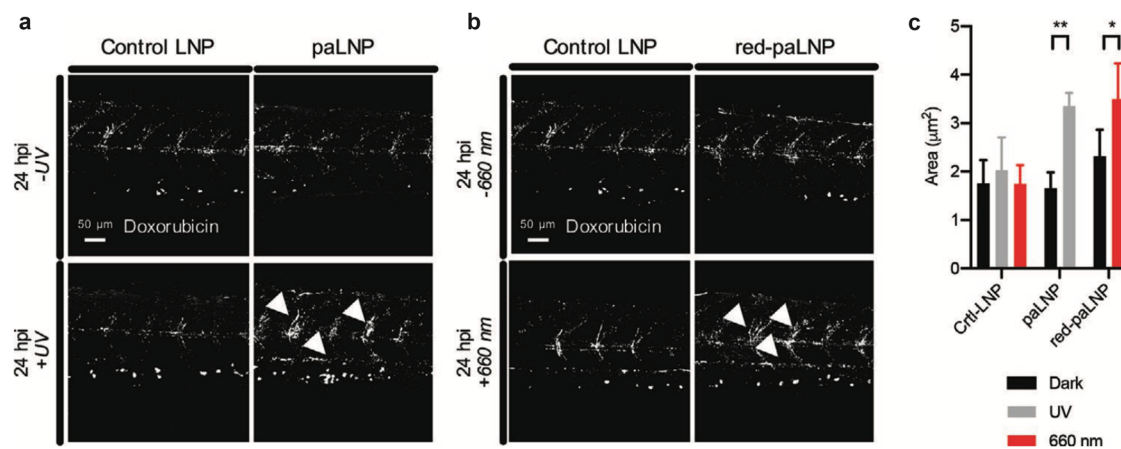


Fig. 7 | Doxorubicin release in zebrafish embryos with and without pulsed light triggers. At 48 h post-fertilization, wild-type zebrafish embryos were intravenously injected with either control lipid nanoparticles (LNPs) or photoactivatable LNPs (with *azo-PC* (paLNP) or *red-azo-PC* (red-paLNP)), both containing Dox (2 nL of a 3 mg/mL solution). After 24 h, the embryos were exposed to pulsed UV-A (365 nm) or deep-red light (660 nm). **a, b** Confocal images of the tail region were acquired to

assess Dox release (white signal) with and without light exposure. White arrows point to areas with enhanced Dox release. **c** Presents quantitative image analysis of Dox release; error bars represent the standard error of the mean (SEM), with significance levels indicated by * $p < 0.1$ and ** $p < 0.01$. Reprinted (adapted) with permission from *Small* 2021, 17, 21, 11⁹⁶. Copyright 2021 John Wiley and Sons under license 5897691312413.

advance their development for clinical trials and eventual medical applications.

Hemithioindigo-modified diacylglycerophospholipids

Hemithioindigos (HTIs) are a relatively unexplored class of photoswitches compared to azobenzenes, despite their unique physical and photophysical characteristics⁹⁹. HTIs consist of an asymmetrical structure combining a thioindigo moiety and a stilbene fragment linked by a central double bond (Fig. 2b). This bond can be photoisomerized between *Z* and *E* configurations, with *Z* being thermodynamically stable and *E* metastable⁹⁹. In a simplified view, the excited state potential energy surface of photoexcited HTI involves two excited states (S_1 and S_2) that interact at a specific geometry, approximately a 90° rotation of the central double bond. This interaction creates a barrier that influences the rate of photoisomerization. Beyond this barrier, a conical intersection connects the excited state and the ground state at the 90° rotation. The remaining 90° rotation occurs on the ground state (S_0) potential energy surface, resulting in the formation of either the *Z* or *E* isomer.

One notable property of HTIs is their light absorption at longer wavelengths compared to unsubstituted azobenzene, which allows photoisomerization under visible light in both directions. Coupled with high fatigue resistance and enhanced thermal bistability, these properties make HTIs particularly promising for biological and materials science applications. Furthermore, substituents at the *para*-position of the sulfur atom significantly influence HTI's photophysical behaviors and photoisomerization kinetics, offering avenues to tailor HTIs with innovative properties.

A synthesis route for hemithioindigo-containing photolipids was detailed by Montoya Pelaez, Eggers and co-workers^{100,101}. This method involves bis-esterification of phosphoglycerol using a key intermediate: hemithioindigo carboxylic acid, which is synthesized via Knoevenagel condensation of a substituted thioindoxyl and a benzaldehyde derivative. The thioindoxyl is derived from a halo-substituted thiophenol and an acrylate through a sequence of Heck coupling, reduction, and Friedel-Crafts acylation-cyclization. The HTI-photolipid derivatives that were reported to date are summarized in Table 2.

It was demonstrated that HTI-photolipids can form stable vesicles that retain photoswitching capabilities within a membrane environment. Meanwhile, a proof-of-concept study showed that photocontrol of vesicle fusion could be achieved through HTI-photolipid isomerization. However, comprehensive investigations into the photophysical properties of

HTI-containing phospholipids in membrane settings are still needed to fully realize their potential for optical membrane control using visible light. The red-shifted switching wavelengths of these photolipids make them intriguing candidates for further exploration in biological and medical applications.

We would like to note that, beyond azobenzenes and hemithioindigo, other photoswitchable and photosensitive units such as stilbenes^{102–104}, tolan¹⁰⁵, and porphyrin¹⁰⁶ have been incorporated into the hydrophobic region of diacylglycerophospholipids. These compounds are promising, demonstrating photoswitching capabilities. They have not yet shown reversible control of membrane properties solely through light exposure, but represent potential avenues for future research.

Future perspective

Photoswitchable diacylglycerophospholipids are a promising innovation with potential across various fields, including, photopharmacology, synthetic biology, and biotechnology. Their ability to undergo light-induced isomerization and reversibly change their lipid footprint offers optical control over cellular processes, highlighting their potential as tools in both laboratory assays and medical applications.

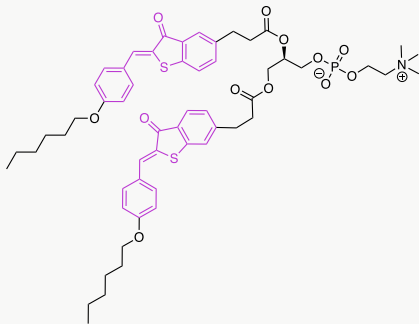
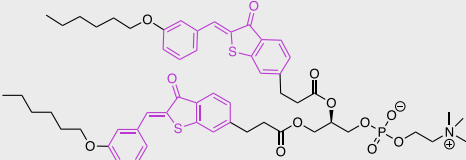
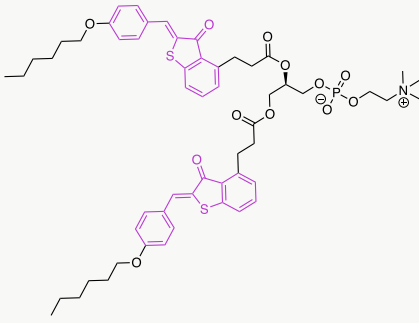
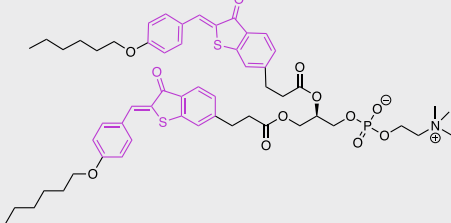
Innovations in photopharmacology

Photopharmacology employs molecular photoswitches to control biological functions with spatial and temporal specificity using light. Photoswitchable diacylglycerophospholipids can be designed to interact with drug molecules, cellular membranes, or specific proteins upon illumination, enabling the (de-)activation of biological processes. The chemical approach offers an additional layer of regulation over cellular functions, potentially minimizing off-target effects and reducing systemic toxicity, thus revolutionizing personalized medicine. Beyond drug delivery, photolipids can alter membrane properties when exposed to light, providing specific control over various cellular responses. Future research should focus on developing diverse libraries of photolipids for tailored applications in photopharmacology.

Photolipids in synthetic biology and biotechnology

Photolipids provide optical control over membrane fusion and vesicle engulfment, essential for many biological processes. Light-induced changes can trigger or inhibit fusion, allowing for on-demand assembly of synthetic compartments, which has great potential for creating artificial cells, synthetic neural networks, biosensors, and responsive materials.

Table 2 | Hemithioindigo-modified phospholipids

Name/ Ref	Chemical structure	Application
PC-HT-6		Vesicle formation and fusion ^{100,101}
PC-HT- <i>m</i> -6		Vesicle formation and fusion ^{100,101}
PC- <i>m'</i> -HT-6		Vesicle formation and fusion ^{100,101}
PC- <i>m</i> -HT-6		Vesicle formation and fusion ^{100,101}

Names and chemical structures of reported HTI-modified diacylglycerophospholipids and their applications.

Technological integration, challenges, and immunogenicity considerations in medical applications

Integrating photoswitchable diacylglycerophospholipids with technologies like CRISPR/Cas and drug delivery systems could enhance precision medicine. For example, CRISPR-Cas9 components (such as Cas9 protein and guide ribonucleic acid (RNA)) could be encapsulated in photoswitchable LNPs that remain inert until activated by specific wavelengths of light and triggering the release of their cargo at the target site. However, challenges include delivering light to target tissues, especially in deeper areas. Advances in light delivery systems and designing photoswitches activated by deep-tissue-penetrating light will be crucial¹⁰⁷. Furthermore, incorporating photolipids into living organisms requires effective strategies, but obstacles persist. Liposome fusion delivers photolipids to membranes but may struggle with efficiency and specificity. Direct incubation integrates lipids into membranes via exchange, though uptake can be limited, and cytotoxicity is a concern. For in vivo use, delivery vehicles like LNPs or hydrogels can transport and protect photolipids, but they are complex to design. Metabolic incorporation offers a natural solution, though it depends on available precursors and

pathways. Also, ensuring the stability and biocompatibility of photolipids under physiological conditions is essential. Rigorous in vivo testing for pharmacokinetics, biodistribution, and potential immunogenicity is necessary. The immune system can recognize certain lipids as foreign, potentially affecting the safety of lipid-based therapies¹⁰⁸. For example, specific lipids in messenger RNA (mRNA) vaccine liposomes, such as those for COVID-19, may cause adverse reactions¹⁰⁹. Additionally, the ethical implications and long-term safety of using these lipids in humans must be carefully addressed.

Conclusion

In conclusion, the complex interplay of lipid composition, structure, and environmental interactions within cellular membranes presents a frontier rich with potential for scientific exploration and technological innovation. Significant progress has been made with azobenzene-modified diacylglycerophospholipids, which allow precise manipulation of membrane behavior using light. These photolipids enable reversible optical control over membrane properties and underscore the need for developing alternative photolipids that could introduce new functionalities, address current limitations, and lead to improved or novel photolipid mechanisms. Although

the application of photolipids in living systems is still emerging, their ability to modulate key biological processes holds much promise. Future research will benefit from a deeper understanding of photolipid dynamics in more complex biological systems to fully harness their potential for biological studies and, ultimately, therapeutic applications. Furthermore, the integration of new photoswitchable units and the refinement of existing systems will expand the scope of membrane-based technologies, paving the way for novel strategies in fields such as photopharmacology, synthetic biology, and biotechnology.

Data availability

No datasets were generated or analyzed during the current study. Figure contents are reproduced with copyright permissions.

Received: 16 July 2024; Accepted: 7 March 2025;

Published online: 01 April 2025

References

- Jacobson, K., Sheets, E. D. & Simson, R. Revisiting the fluid mosaic model of membranes. *Science* **268**, 1441–1442 (1995).
- Singer, S. in *Structure of Biological Membranes* (Springer, 1977).
- Stieger, B., Steiger, J. & Locher, K. P. Membrane lipids and transporter function. *Biochim. Biophys. Acta Mol. Basis Dis.* **1867**, 166079 (2021).
- Doktorova, M., Symons, J. L. & Levental, I. Structural and functional consequences of reversible lipid asymmetry in living membranes. *Nat. Chem. Biol.* **16**, 1321–1330 (2020).
- Dingjan, T. & Futerman, A. H. The fine-tuning of cell membrane lipid bilayers accentuates their compositional complexity. *Bioessays* **43**, 2100021 (2021).
- Sych, T., Levental, K. R. & Sezgin, E. Lipid–protein interactions in plasma membrane organization and function. *Annu. Rev. Biophys.* **51**, 135–156 (2022).
- van Meer, G. Cellular lipidomics. *EMBO J.* **24**, 3159–3165–3165 (2005).
- Coskun, Ü. & Simons, K. Cell membranes: the lipid perspective. *Structure* **19**, 1543–1548 (2011).
- Dowhan, W. The role of phospholipids in cell function. *Adv. Lipobiol.* **2**, 79–107 (1997).
- Fadeel, B. & Xue, D. The ins and outs of phospholipid asymmetry in the plasma membrane: roles in health and disease. *Crit. Rev. Biochem. Mol. Biol.* **44**, 264–277 (2009).
- Huster, D., Maiti, S. & Herrmann, A. Phospholipid membranes as chemically and functionally tunable materials. *Adv. Mater.* **36**, 2312898 (2024).
- Han, X. Lipidomics for studying metabolism. *Nat. Rev. Endocrinol.* **12**, 668–679 (2016).
- Yéagle, P. L. Lipid regulation of cell membrane structure and function. *FASEB J.* **3**, 1833–1842 (1989).
- Harayama, T. & Riezman, H. Understanding the diversity of membrane lipid composition. *Nat. Rev. Mol. Cell Biol.* **19**, 281–296 (2018).
- Brown, M. F. Curvature forces in membrane lipid–protein interactions. *Biochemistry* **51**, 9782–9795 (2012).
- Whited, A. M. & Johs, A. The interactions of peripheral membrane proteins with biological membranes. *Chem. Phys. Lipids* **192**, 51–59 (2015).
- Renne, M. F. & Ernst, R. Membrane homeostasis beyond fluidity: control of membrane compressibility. *Trends Biochem. Sci.* **48**, 963–977 (2023).
- Chan, Y.-H. M. & Boxer, S. G. Model membrane systems and their applications. *Curr. Opin. Chem. Biol.* **11**, 581–587 (2007).
- Feller, S. E. Molecular dynamics simulations of lipid bilayers. *Curr. Opin. Colloid Interface Sci.* **5**, 217–223 (2000).
- Penno, A., Hackenbroich, G. & Thiele, C. Phospholipids and lipid droplets. *Biochim. Biophys. Acta Mol. Cell Biol. Lipids* **1831**, 589–594 (2013).
- Valentine, W. J., Hashidate–Yoshida, T., Yamamoto, S. & Shindou, H. Biosynthetic enzymes of membrane glycerophospholipid diversity as therapeutic targets for drug development. *Adv. Exp. Med. Biol.* **1274**, 5–27 (2020).
- Gawrisch, K., Eldho, N. V. & Holte, L. L. The structure of DHA in phospholipid membranes. *Lipids* **38**, 445–452 (2003).
- Holte, L. L., Peter, S. A., Sinnwell, T. M. & Gawrisch, K. 2H nuclear magnetic resonance order parameter profiles suggest a change of molecular shape for phosphatidylcholines containing a polyunsaturated acyl chain. *Biophys. J.* **68**, 2396–2403 (1995).
- Lentz, B. R. Exposure of platelet membrane phosphatidylserine regulates blood coagulation. *Prog. Lipid Res.* **42**, 423–438 (2003).
- Veldhuizen, R., Nag, K., Orgeig, S. & Possmayer, F. The role of lipids in pulmonary surfactant. *Biochim. Biophys. Acta* **1408**, 90–108 (1998).
- Mason, T. M. The role of factors that regulate the synthesis and secretion of very-low-density lipoprotein by hepatocytes. *Crit. Rev. Clin. Lab. Sci.* **35**, 461–487 (1998).
- Rodríguez-Cuenca, S., Pellegrinelli, V., Campbell, M., Oresic, M. & Vidal-Puig, A. Sphingolipids and glycerophospholipids – The “ying and yang” of lipotoxicity in metabolic diseases. *Prog. Lipid Res.* **66**, 14–29 (2017).
- Zeng, C. et al. Lipidomics profiling reveals the role of glycerophospholipid metabolism in psoriasis. *Gigascience* **6**, 1–11 (2017).
- Farooqui, A. A., Horrocks, L. A. & Farooqui, T. Glycerophospholipids in brain: their metabolism, incorporation into membranes, functions, and involvement in neurological disorders. *Chem. Phys. Lipids* **106**, 1–29 (2000).
- Frisardi, V., Panza, F., Seripa, D., Farooqui, T. & Farooqui, A. A. Glycerophospholipids and glycerophospholipid-derived lipid mediators: a complex meshwork in Alzheimer’s disease pathology. *Prog. Lipid Res.* **50**, 313–330 (2011).
- Dorninger, F., Forss-Petter, S. & Berger, J. From peroxisomal disorders to common neurodegenerative diseases—the role of ether phospholipids in the nervous system. *FEBS Lett.* **591**, 2761–2788 (2017).
- Socrier, L. & Steinem, C. Photo-lipids: light-sensitive nano-switches to control membrane properties. *Chempluschem* **88**, e202300203 (2023).
- Morstein, J., Impastato, A. C. & Trauner, D. Photoswitchable lipids. *ChemBiochem* **22**, 73–83 (2021).
- Brieke, C., Rohrbach, F., Gottschalk, A., Mayer, G. & Heckel, A. Light-controlled tools. *Angew. Chem., Int. Ed.* **51**, 8446–8476 (2012).
- Trauner, D. & Morstein, J. Optical control of glycerolipids and sphingolipids. *Chimia* **75**, 1022–1022 (2021).
- Bennett, D. E., Lamparski, H. & O’Brien, D. F. Photosensitive liposomes. *J. Liposome Res.* **4**, 331–348 (1994).
- Szymanski, W., Beierle, J. M., Kistemaker, H. A., Velema, W. A. & Feringa, B. L. Reversible photocontrol of biological systems by the incorporation of molecular photoswitches. *Chem. Rev.* **113**, 6114–6178 (2013).
- Beharry, A. A. & Woolley, G. A. Azobenzene photoswitches for biomolecules. *Chem. Soc. Rev.* **40**, 4422–4437 (2011).
- Shang, T., Smith, K. A. & Hatton, T. A. Photoresponsive surfactants exhibiting unusually large, reversible surface tension changes under varying illumination conditions. *Langmuir* **19**, 10764–10773 (2003).
- Roy, D. S. et al. Membrane-mediated allosteric action of serotonin on a noncognate G-protein-coupled receptor. *J. Phys. Chem. Lett.* **15**, 1711–1718 (2024).
- Marturano, V. et al. Modeling of azobenzene-based compounds. *Phys. Sci. Rev.* **18**, 2479–2482 (2017).
- Hartley, G. S. The cis-form of azobenzene. *Nature* **140**, 281–281 (1937).
- Wu, S. & Butt, H.-J. Solar-thermal energy conversion and storage using photoresponsive azobenzene-containing polymers. *Macromol. Rapid Commun.* **41**, 1900413 (2020).
- Lerch, M. M., Hansen, M. J., van Dam, G. M., Szymanski, W. & Feringa, B. L. Emerging targets in photopharmacology. *Angew. Chem.* **55**, 10978–10999 (2016).

45. Aleotti, F. et al. Multidimensional potential energy surfaces resolved at the RASPT2 level for accurate photoinduced isomerization dynamics of azobenzene. *J. Chem. Theory Comput.* **15**, 6813–6823 (2019).
46. Cusati, T., Granucci, G. & Persico, M. Photodynamics and time-resolved fluorescence of azobenzene in solution: a mixed quantum-classical simulation. *J. Am. Chem. Soc.* **133**, 5109–5123 (2011).
47. Quick, M. et al. Photoisomerization dynamics and pathways of trans- and cis-azobenzene in solution from broadband femtosecond spectroscopies and calculations. *J. Phys. Chem. B* **118**, 8756–8771 (2014).
48. Tan, E. M. M. et al. Fast photodynamics of azobenzene probed by scanning excited-state potential energy surfaces using slow spectroscopy. *Nat. Commun.* **6**, 5860 (2015).
49. Casellas, J., Bearpark, M. J. & Reguero, M. Excited-state decay in the photoisomerisation of azobenzene: a new balance between mechanisms. *Chemphyschem* **17**, 3068–3079 (2016).
50. Cantatore, V., Granucci, G. & Persico, M. Simulation of the $\pi \rightarrow \pi^*$ photodynamics of azobenzene: Decoherence and solvent effects. *Comput. Theor. Chem.* **1040–1041**, 126–135 (2014).
51. Titov, E., Granucci, G., Götze, J. P., Persico, M. & Saalfrank, P. Dynamics of azobenzene dimer photoisomerization: electronic and steric effects. *J. Phys. Chem. Lett.* **7**, 3591–3596 (2016).
52. Cembran, A., Bernardi, F., Garavelli, M., Gagliardi, L. & Orlandi, G. On the mechanism of the cis–trans isomerization in the lowest electronic states of azobenzene: S0, S1, and T1. *J. Am. Chem. Soc.* **126**, 3234–3243 (2004).
53. Gagliardi, L., Orlandi, G., Bernardi, F., Cembran, A. & Garavelli, M. A theoretical study of the lowest electronic states of azobenzene: the role of torsion coordinate in the cis–trans photoisomerization. *Theor. Chem. Acc.* **111**, 363–372 (2004).
54. Monti, S., Gardini, E., Bortolus, P. & Amouyal, E. The triplet state of azobenzene. *Chem. Phys. Lett.* **77**, 115–119 (1981).
55. Goulet-Hanssens, A. et al. Electrocatalytic Z \rightarrow E isomerization of azobenzenes. *J. Am. Chem. Soc.* **139**, 335–341 (2017).
56. Garcia-Amorós, J., Sánchez-Ferrer, A., Massad, W. A., Nonell, S. & Velasco, D. Kinetic study of the fast thermal cis-to-trans isomerisation of para-, ortho- and polyhydroxyazobenzenes. *Phys. Chem. Chem. Phys.* **12**, 13238–13242 (2010).
57. Bandara, H. M. D. & Burdette, S. C. Photoisomerization in different classes of azobenzene. *Chem. Soc. Rev.* **41**, 1809–1825 (2012).
58. Bléger, D., Schwarz, J., Brouwer, A. M. & Hecht, S. o-Fluoroazobenzenes as readily synthesized photoswitches offering nearly quantitative two-way isomerization with visible light. *J. Am. Chem. Soc.* **134**, 20597–20600 (2012).
59. Konrad, D. B. et al. Computational design and synthesis of a deeply red-shifted and bistable azobenzene. *J. Am. Chem. Soc.* **142**, 6538–6547 (2020).
60. Sandhu, S. S., Yianni, Y. P., Morgan, C. G., Taylor, D. M. & Zaba, B. The formation and Langmuir-Blodgett deposition of monolayers of novel photochromic azobenzene-containing phospholipid molecules. *Biochim. Biophys. Acta Biomembr.* **860**, 253–262 (1986).
61. Song, X., Perlstein, J. & Whitten, D. G. Supramolecular aggregates of azobenzene phospholipids and related compounds in bilayer assemblies and other microheterogeneous media: structure, properties, and photoreactivity. *J. Am. Chem. Soc.* **119**, 9144–9159 (1997).
62. Morgan, C. G., Thomas, E. W., Yianni, Y. P. & Sandhu, S. S. Incorporation of a novel photochromic phospholipid molecule into vesicles of dipalmitoylphosphatidylcholine. *Biochim. Biophys. Acta Biomembr.* **820**, 107–114 (1985).
63. Pritzl, S. D. et al. Postsynthetic photocontrol of giant liposomes via fusion-based photolipid doping. *Langmuir* **38**, 11941–11949 (2022).
64. Urban, P. et al. Light-controlled lipid interaction and membrane organization in photolipid bilayer vesicles. *Langmuir* **34**, 13368–13374 (2018).
65. Pritzl, S. D. et al. Optical membrane control with red light enabled by red-shifted photolipids. *Langmuir* **38**, 385–393 (2021).
66. Pernpeintner, C. & Lohmüller, T. et al. Light-controlled membrane mechanics and shape transitions of photoswitchable lipid vesicles. *Langmuir* **33**, 4083–4089 (2017).
67. Johnson, T. G., Sadeghi-Kelishadi, A. & Langton, M. J. A photo-responsive transmembrane anion transporter relay. *J. Am. Chem. Soc.* **144**, 10455–10461 (2022).
68. Tei, R., Morstein, J., Shemet, A., Trauner, D. & Baskin, J. M. Optical control of phosphatidic acid signaling. *ACS Cent. Sci.* **7**, 1205–1215 (2021).
69. Kuiper, J. M. & Engberts, J. B. H-aggregation of azobenzene-substituted amphiphiles in vesicular membranes. *Langmuir* **20**, 1152–1160 (2004).
70. Kuiper, J. M., Hulst, R. & Engberts, J. B. A selective and mild synthetic route to dialkyl phosphates. *Synthesis* **2003**, 0695–0698 (2003).
71. Backus, E. H., Kuiper, J. M., Engberts, J. B., Poolman, B. & Bonn, M. Reversible optical control of monolayers on water through photoswitchable lipids. *J. Phys. Chem. B* **115**, 2294–2302 (2011).
72. Folgering, J. H. A., Kuiper, J. M., de Vries, A. H., Engberts, J. B. F. N. & Poolman, B. Lipid-mediated light activation of a mechanosensitive channel of large conductance. *Langmuir* **20**, 6985–6987 (2004).
73. Morgan, C. G., Sandhu, S. S., Yianni, Y. P. & Dodd, N. J. F. The phase behaviour of dispersions of Bis-Azo PC: photoregulation of bilayer dynamics via lipid photochromism. *Biochim. Biophys. Acta Biomembr.* **903**, 495–503 (1987).
74. Morgan, C. G., Thomas, E. W., Sandhu, S. S., Yianni, Y. P. & Mitchell, A. C. Light-induced fusion of liposomes with release of trapped marker dye is sensitised by photochromic phospholipid. *Biochim. Biophys. Acta Biomembr.* **903**, 504–509 (1987).
75. Morgan, C. G., Yianni, Y. P., Sandhu, S. S. & Mitchell, A. C. Liposome fusion and lipid exchange on ultraviolet irradiation of liposomes containing a photochromic phospholipid. *Photochem. Photobiol.* **62**, 24–29 (1995).
76. Bisby, R. H., Mead, C. & Morgan, C. G. Wavelength-programmed solute release from photosensitive liposomes. *Biochem. Biophys. Res. Commun.* **276**, 169–173 (2000).
77. Bisby, R. H., Mead, C. & Morgan, C. G. Photosensitive liposomes as ‘cages’ for laser-triggered solute delivery: the effect of bilayer cholesterol on kinetics of solute release. *FEBS Lett.* **463**, 165–168 (1999).
78. Morgan, C. G., Bisby, R. H., Johnson, S. A. & Mitchell, A. C. Fast solute release from photosensitive liposomes: an alternative to ‘caged’ reagents for use in biological systems. *FEBS Lett.* **375**, 113–116 (1995).
79. Bisby, R. H., Mead, C., Mitchell, A. C. & Morgan, C. G. Fast laser-induced solute release from liposomes sensitized with photochromic lipid: effects of temperature, lipid host, and sensitizer concentration. *Biochem. Biophys. Res. Commun.* **262**, 406–410 (1999).
80. Morgan, C. G., Mitchell, A. & Chowdhary, R. Photosensitive liposomes as potential drug delivery vehicles for photodynamic therapy. In *Future Trends in Biomedical Applications of Lasers* (SPIE, 1991).
81. Bisby, R. H., Morgan, C. G. & Munro, L. H. Control of pro-oxidant activity of cupric ions by entrapment in unilamellar lipid vesicles. *Free Radic. Res. Commun.* **16**, 65–71 (1992).
82. Urban, P. et al. A lipid photoswitch controls fluidity in supported bilayer membranes. *Langmuir* **36**, 2629–2634 (2020).
83. Crea, F. et al. Photoactivation of a mechanosensitive channel. *Front. Mol. Biosci.* **9**, 905306 (2022).
84. Pritzl, S. D. et al. Photolipid bilayer permeability is controlled by transient pore formation. *Langmuir* **36**, 13509–13515 (2020).
85. Klaja, O., Frank, J. A., Trauner, D. & Bondar, A. N. Potential energy function for a photo-switchable lipid molecule. *J. Comput. Chem.* **41**, 2336–2351 (2020).
86. Manafirad, A. et al. Structural and mechanical response of two-component photoswitchable lipid bilayer vesicles. *Langmuir* **39**, 15932–15941 (2023).

87. Heimburg, T. Lipid ion channels. *Biophys. Chem.* **150**, 2–22 (2010).
88. Doroudgar, M., Morstein, J., Becker-Baldus, J., Trauner, D. & Glaubitz, C. How photoswitchable lipids affect the order and dynamics of lipid bilayers and embedded proteins. *J. Am. Chem. Soc.* **143**, 9515–9528 (2021).
89. Scheidt, H. A. et al. Light-induced lipid mixing implies a causal role of lipid splay in membrane fusion. *Biochim. Biophys. Acta Biomembr.* **1862**, 183438 (2020).
90. Mangiarotti, A., Aleksanyan, M., Siri, M., Lipowsky, R. & Dimova, R. Photoswitchable endocytosis of biomolecular condensates in giant vesicles. *Adv. Sci.* **11**, 2198–3844 (2024).
91. Ober, M. F. et al. SAXS measurements of azobenzene lipid vesicles reveal buffer-dependent photoswitching and quantitative Z → E isomerisation by X-rays. *Nanophotonics* **11**, 2361–2368 (2022).
92. Pritzl, S. D. *Optical Nanoagents in Phospholipid Membranes: Controlling Bilayer Properties with Light*. Ludwig-Maximilians-Universität München, 2021.
93. Aleksanyan, M. et al. Photomanipulation of minimal synthetic cells: area increase, softening, and interleaflet coupling of membrane models doped with azobenzene-lipid photoswitches. *Adv. Sci.* **10**, 2198–3844 (2023).
94. Haswell, E. S., Phillips, R. & Rees, D. C. Mechanosensitive channels: what can they do and how do they do it? *Structure* **19**, 1356–1369 (2011).
95. Jiménez-Rojo, N. et al. Optical control of membrane fluidity modulates protein secretion. Preprint at *bioRxiv* 2022.2002. 2014.480333 (2022).
96. Chandler, N. et al. Optimized photoactivatable lipid nanoparticles enable red light triggered drug release. *Small* **17**, 2008198 (2021).
97. Xiong, H. et al. Optical control of neuronal activities with photoswitchable nanovesicles. *Nano Res.* **16**, 1033–1041 (2023).
98. Simon, J., Schwalm, M., Morstein, J., Trauner, D. & Jasanoff, A. Mapping light distribution in tissue by using MRI-detectable photosensitive liposomes. *Nat. Biomed. Eng.* **7**, 313–322 (2023).
99. Wiedbrauk, S. & Dube, H. Hemithioindigo—an emerging photoswitch. *Tetrahedron Lett.* **56**, 4266–4274 (2015).
100. Eggers, K., Fyles, T. M. & Montoya-Pelaez, P. J. Synthesis and characterization of photoswitchable lipids containing hemithioindigo chromophores. *J. Org. Chem.* **66**, 2966–2977 (2001).
101. Montoya Pelaez, P. J. Design and synthesis of hemithioindigo lipids for photo-controlled membrane fusion. Doctoral dissertation, University of Victoria, Canada (1999).
102. Whitten, D. G. Photochemistry and photophysics of trans-stilbene and related alkenes in surfactant assemblies. *Acc. Chem. Res.* **26**, 502–509 (1993).
103. Song, X., Geiger, C., Leinhos, U., Perlstein, J. & Whitten, D. G. trans-Stilbene aggregates in microheterogeneous media: evidence for a chiral cyclic supramolecular unit. *J. Am. Chem. Soc.* **116**, 10340–10341 (1994).
104. Song, X., Geiger, C., Furman, I. & Whitten, D. G. Anatomy of an aggregate. use of functionalized phospholipids to investigate stoichiometry and structure of ^mHⁿ aggregates formed from amphiphilic trans-stilbene derivatives. *J. Am. Chem. Soc.* **116**, 4103–4104 (1994).
105. Farahat, C. W., Penner, T. L., Ulman, A. & Whitten, D. G. Enhanced aggregation of derivatized tolan surfactants through donor–acceptor interactions at the air–water interface and in Langmuir–Blodgett films. *J. Phys. Chem.* **100**, 12616–12623 (1996).
106. Kilian, H. I. et al. Light-triggered release of large biomacromolecules from porphyrin-phospholipid liposomes. *Langmuir* **37**, 10859–10865 (2021).
107. Morstein, J. & Trauner, D. New players in phototherapy: photopharmacology and bio-integrated optoelectronics. *Curr. Opin. Chem. Biol.* **50**, 145–151 (2019).
108. Verbeke, R., Lentacker, I., De Smedt, S. C. & Dewitte, H. Three decades of messenger RNA vaccine development. *Nano Today* **28**, 100766 (2019).
109. Buschmann, M. D. et al. Nanomaterial delivery systems for mRNA vaccines. *Vaccine* **9**, 65 (2021).

Acknowledgements

This work was supported by the European Research Council through the Consolidator grant “ProForce”, the National Institute of Health (NIH, United States) through an R01 grant (GM126228/GM/NIGMS), and the Deutsche Forschungsgemeinschaft (DFG) through the Collaborative Research Center SFB1032 (Project No. 201269156, Project A8). S.D.P. was further supported by the Alexander-von-Humboldt Foundation through a Feodor-Lynen fellowship.

Author contributions

S.D.P. conceived and structured the review and wrote the initial manuscript draft. J.M. and N.A.P. contributed to the literature collection and conceptualization. All authors (S.D.P., J.M., N.A.P., J.L., T.L., and D.H.T.) participated in the editing and review process, and manuscript refinement. J.L., T.L., and D.H.T. provided supervision and secured funding.

Competing interests

The authors declare no competing interests.

Additional information

Supplementary information The online version contains supplementary material available at <https://doi.org/10.1038/s43246-025-00773-8>.

Correspondence and requests for materials should be addressed to Stefanie D. Pritzl.

Peer review information *Communications Materials* thanks Andreas Herrmann and the other, anonymous, reviewer(s) for their contribution to the peer review of this work. Primary Handling Editors: Jet-Sing Lee.

Reprints and permissions information is available at <http://www.nature.com/reprints>

Publisher's note Springer Nature remains neutral with regard to jurisdictional claims in published maps and institutional affiliations.

Open Access This article is licensed under a Creative Commons Attribution-NonCommercial-NoDerivatives 4.0 International License, which permits any non-commercial use, sharing, distribution and reproduction in any medium or format, as long as you give appropriate credit to the original author(s) and the source, provide a link to the Creative Commons licence, and indicate if you modified the licensed material. You do not have permission under this licence to share adapted material derived from this article or parts of it. The images or other third party material in this article are included in the article's Creative Commons licence, unless indicated otherwise in a credit line to the material. If material is not included in the article's Creative Commons licence and your intended use is not permitted by statutory regulation or exceeds the permitted use, you will need to obtain permission directly from the copyright holder. To view a copy of this licence, visit <http://creativecommons.org/licenses/by-nc-nd/4.0/>.

© The Author(s) 2025